

Article

Chemical Constituents of the Leaves of Butterbur (*Petasites japonicus*) and Their Anti-Inflammatory Effects

Jin Su Lee ¹, Miran Jeong ², Sangsu Park ³, Seung Mok Ryu ⁴, Jun Lee ⁴ , Ziteng Song ⁵, Yuanqiang Guo ⁵, Jung-Hye Choi ^{1,2}, Dongho Lee ^{6,*} and Dae Sik Jang ^{1,2,*} 

¹ Department of Life and Nanopharmaceutical Sciences, Graduate School, Kyung Hee University, Seoul 02447, Korea; lee2649318@naver.com (J.S.L.); jchoi@khu.ac.kr (J.-H.C.)

² College of Pharmacy, Kyung Hee University, Seoul 02447, Korea; jeongmiran@hanmail.net

³ Department of Fundamental Pharmaceutical Sciences, Graduate School, Kyung Hee University, Seoul 02447, Korea; x-zara@nate.com

⁴ Herbal Medicine Resources Research Center, Korea Institute of Oriental Medicine, Jeollanam-do 58245, Korea; smryu@kiom.re.kr (S.M.R.); junlee@kiom.re.kr (J.L.)

⁵ State Key Laboratory of Medicinal Chemical Biology, College of Pharmacy, Tianjin Key Laboratory of Molecular Drug Research, and Drug Discovery Center for Infectious Disease, Nankai University, Tianjin 300350, China; kdszt152@163.com (Z.S.); victgyq@nankai.edu.cn (Y.G.)

⁶ Department of Biosystems and Biotechnology, College of Life Sciences and Biotechnology, Korea University, Seoul 02841, Korea

* Correspondence: dongholee@korea.ac.kr (D.L.); dsjang@khu.ac.kr (D.S.J.); Tel.: +82-2-3290-3017 (L.D.); +82-2-961-0719 (D.S.J.)

Received: 30 October 2019; Accepted: 27 November 2019; Published: 29 November 2019



Abstract: Two new aryltetralin lactone lignans, petasitesins A and B were isolated from the hot water extract of the leaves of butterbur (*Petasites japonicus*) along with six known compounds. The chemical structures of lignans **1** and **2** were elucidated on the basis of 1D and 2D nuclear magnetic resonance (NMR) spectroscopic data, electronic circular dichroism (ECD) and vibrational circular dichroism (VCD) spectra. Petasitesin A and cimicifugic acid D showed significant inhibitory effects on the production of both prostaglandin E₂ (PGE₂) and NO in RAW264.7 macrophages. The expressions of inducible nitric oxide synthase (iNOS) and cyclooxygenase-2 (COX-2) were inhibited by compound **1** in RAW264.7 cells. Furthermore, compounds **1** and **3** exhibited strong affinities with both iNOS and COX-2 enzymes in molecular docking studies.

Keywords: *Petasites japonicus*; Asteraceae; lignan; anti-inflammation; NO; PGE₂; iNOS; COX-2; molecular docking

1. Introduction

Petasites japonicus Maxim (Asteraceae), known as butterbur, Japanese butterbur, and giant butterbur, is used as a botanical dietary supplement in the USA. The aerial parts of *P. japonicus* have been used in traditional Japanese folk medicine as an antipyretic, antitussive, or wound healing agent [1]. The constituents of *P. japonicus* have been reported and include flavonoids [2], sesquiterpenes [3–5], triterpenes [6], and various types of phenolic compounds [7]. Moreover, the leaves or stalks of *P. japonicus* are commonly consumed as vegetables in Korea and Japan. In the course of searching for active compounds from higher plants [8,9], the leaves of *P. japonicus* were selected for a detailed study since a hot water extract of the leaves of *P. japonicus* have shown inhibitory activity against nitric oxide (NO) production in RAW 264.7 cells [half maximal inhibitory concentration (IC₅₀) value:

19 ± 4.9 µg/mL]. Phytochemical study on the hot water extract resulted in the isolation of two new aryltetralin lactone lignans (**1** and **2**) along with six previously known compounds (Figure 1). The chemical structures of the new lignans **1** and **2** were determined by interpretation of 1D and 2D nuclear magnetic resonance (NMR) spectroscopic data, and by electronic circular dichroism (ECD) and vibrational circular dichroism (VCD) studies.

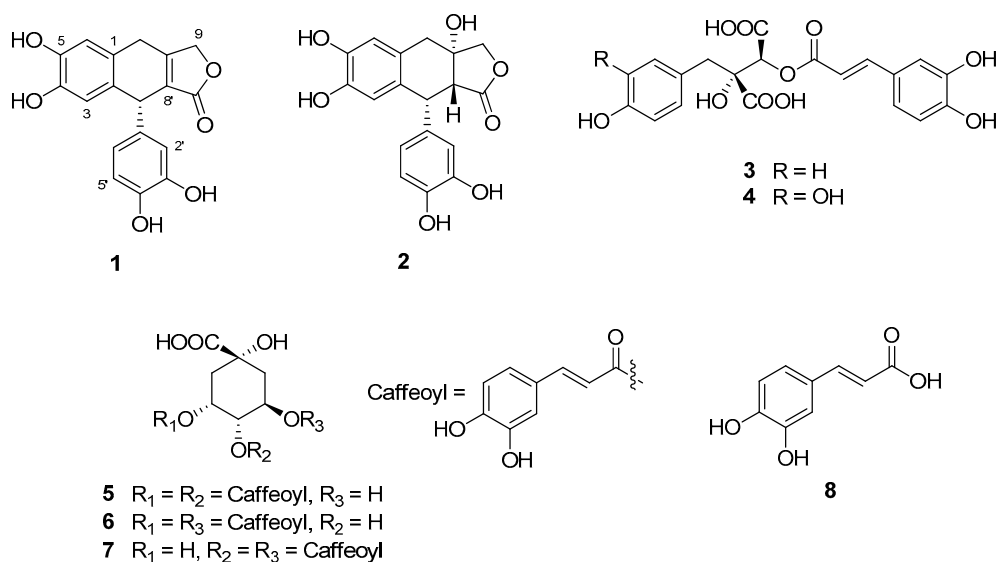


Figure 1. Chemical structures of the isolates 1–8.

All the isolates from the leaves of *P. japonicus* were evaluated for their inhibitory effects on lipopolysaccharide (LPS)-induced production of pro-inflammatory mediators NO and prostaglandin E₂ (PGE₂) in the LPS-stimulated RAW 264.7 macrophages. We describe isolation of the secondary metabolites from the leaves of *P. japonicus*, structure elucidation of the two new lignans (**1** and **2**), and anti-inflammatory effects of the isolates as well as the possible mechanism.

2. Materials and Methods

2.1. General Experimental Procedures

General experimental procedures are described in the Supplementary Materials.

2.2. Plant Material

The leaves of *Petasites japonicus* (Asteraceae) were obtained from Nature Bio Co. (Seoul, Republic of Korea), in October 2016. The plant material was identified by one of the authors (D.S.J.) and the plant specimen (PEJA-2016) has been deposited in the Laboratory of Natural Product Medicine, College of Pharmacy, Kyung Hee University.

2.3. Isolation of Compounds

The dried leaves (500 g) were extracted once with 10 L of boiled water for 4 h and the solvent was evaporated with freeze drying. The extract (100.0 g) was separated over Diaion HP-20 (Mitsubishi, Tokyo, Japan) column eluted with an H₂O-acetone gradient (from 1:0 to 0:1 *v/v*, gradient) to give 15 fractions (K1–K15). A part of fraction K3 was fractionated with medium pressure liquid chromatography (MPLC) using Redi Sep (Teledyne Isco, Lincoln, NE, USA)-C18 cartridge (13 g, acetonitrile–H₂O, 0:1 to 3:7 *v/v*, gradient) and purified by high performance liquid chromatography (HPLC) using YMC Pack ODS-A column (Phenomenex, Torrance, CA, USA), yielding compound **8** (7.7 mg). Fraction K6 was separated over Sephadex LH-20 (Amersham Pharmacia Biotech, Buckinghamshire, United Kingdom) column with an acetone–H₂O mixture (6:4 *v/v*) as solvent to give three fractions (K6-1–K6-3). Fraction

K6-2 was fractionated further using Sephadex LH-20 with an acetone–H₂O mixture (2:8 *v/v*) to yield six subfractions (K6-2-1–K6-2-6). Compound **4** (0.5 g) and **3** (27.1 mg) were obtained from fraction K6-2-4 using LiChroprep RP-18 (Merck, Kenilworth, NJ, USA) CC. Fraction K8 was loaded to Sephadex LH-20 as stationary phase eluting with EtOH–H₂O mixture (1:1 *v/v*) to afford 12 pooled fractions (K8-1–K8-12). Compound **5** (40.3 mg), **6** (4.2 mg), and **7** (4.7 mg) were purified from fraction K8-6 by HPLC with a Luna 10 μ m C18(2) 100 Å column. Subfraction K8-9 was purified using Luna 10 μ m C18 (2) 100 Å column to obtain compound **2** (61.6 mg). Fraction K9 was fractionated further using Sephadex LH-20 column eluted with the EtOH–H₂O mixture (1:1 *v/v*) to generate ten fractions (K9-1–K9-10). Fraction K9-6 was purified by HPLC using YMC Pack ODS-A column, yielding compound **1** (4.2 mg).

2.3.1. Petasitesin A (**1**)

Dark brownish powder; $[\alpha]_D^{23}$: -11.5° (*c* 0.1, MeOH); ultraviolet (UV) (MeOH) λ_{\max} (log ϵ) 204 nm (3.85), 262 nm (3.57); CD (CH₃CN) λ_{\max} 214 (-10.4), 239 (2.1), 254 (-5.3); infrared (IR) (ATR) ν_{\max} 3333, 2915, 2847, 1718, 1524, 1240 cm^{-1} ; High resolution electrospray ionization mass spectrometry (HRESIMS) (HRESIMS) (negative mode) *m/z* 325.0714 [M–H][–] (calculated for C₁₈H₁₃O₆, 325.0712) (Figure S1); ¹H and ¹³C NMR data (Table 1) (Figures S2 and S3); 2D NMR data (Figures S4–S7).

Table 1. ¹H (500 MHz) and ¹³C NMR (125 MHz) data of compounds **1** and **2**.

Position	1 (in Acetone-<i>d</i>₆)		2 (in CD₃OD)	
	δ_C	δ_H Multi (J in Hz)	δ_C	δ_H Multi (J in Hz)
1	129.8		127.0	
2	136.9		130.1	
3	116.9	6.60 s	117.1	6.55 s
4	145.1		145.5	
5	145.3		145.7	
6	115.7	6.72 s	117.0	6.64 s
7	29.0	3.86 d (23.0) 3.62 overlapped	39.6	2.83 d (14.5) 2.67 d (14.5)
8	160.9		78.0	
9	72.4	4.97 d (17.0) 4.89 d (17.0)	80.1	4.17 d (10.0) 3.93 d (10.0)
1'	123.0		135.5	
2'	116.2	6.59 d (2.0)	116.0	6.58 d (2.0)
3'	145.9		146.3	
4'	144.6		144.8	
5'	116.1	6.63 d (8.0)	116.2	6.68 d (8.0)
6'	120.3	6.45 dd (8.0, 2.0)	120.2	6.52 dd (8.0, 2.0)
7'	42.3	4.53 s	47.4	4.18 d (3.0)
8'	128.2		56.2	3.24 d (3.0)
9'	173.9		181.0	

2.3.2. Petasitesin B (**2**)

Dark brownish powder; $[\alpha]_D^{23}$: -20.6° (*c* 0.1, MeOH); UV (MeOH) λ_{\max} (log ϵ) 206 nm (4.34), 287 nm (3.48); CD (CH₃CN) λ_{\max} 203 (4.0), 210 (-5.4), 222 (-4.4), and 229 (1.9); IR (ATR) ν_{\max} 3305, 1768, 1606, 1514 cm^{-1} ; HRESIMS (negative mode) *m/z* 343.0810 [M–H][–] (calculated for C₁₈H₁₅O₇, 343.0818) (Figure S8); ¹H and ¹³C NMR data (Table 1) (Figures S9 and S10); 2D NMR data (Figures S11–S14).

2.4. Computational Methods

ECD and VCD calculations of compounds **1** and **2** were conducted as described previously [10,11]. In brief, their 3D models were built from Chem3D modeling. Conformational analysis was performed by the MMFF force field as implemented in Spartan'14 software (Wavefunction, Inc., Irvine, CA, USA; 2014). Geometrical optimization of the selected conformers was performed at the B3LYP/6–31

+ G (d,p) level by Gaussian 09 software (Revision E.01; Gaussian, Inc., Wallingford, CT, USA; 2009). The theoretical ECD and VCD spectra were calculated at the CAM-B3LYP/SVP level with a CPCM solvent model (acetonitrile) and at the DFT [B3LYP/6–31 + G(d,p)] basis set level by the Gaussian 09 software, respectively.

2.5. Measurement of NO Production

The 3-[4¹⁴C-dimethylthiazol-2-yl]-2,5-dipheyl tetrazolium bromide (MTT) and Griess reaction assays were used for cell viability studies and measuring nitrite levels, respectively, as reported previously [12].

2.6. Measurement of PGE₂

The RAW 264.7 macrophage cell lines were pretreated with various concentrations of the extract and isolates 1–8 for 1 h and then stimulated with or without LPS (1 µg/mL) for 24 h. A selective COX-2 inhibitor, NS-398 (*N*-[2-(cyclohexyloxy)-4-nitrophenyl]methanesulfonamide; Sigma Aldrich, St. Louis, MO, USA) was used as a positive control for blocking PGE₂ production. PGE₂ levels in cell culture mediums were measured using the same methods as described in the previous paper [12].

2.7. Measurement of iNOS and COX-2 Expression

Quantitative polymerase chain reaction (qPCR) using Thermal Cycler Dice Real Time PCR System (Takara Bio Inc., Shiga, Japan) was used to determine the steady-state mRNA levels of inducible nitric oxide synthase (iNOS) and cyclooxygenase-2 (COX-2) as reported previously [12].

2.8. Molecular Docking Studies

The software AutoDock Vina with AutoDock Tools (The Scripps Research Institute, La Jolla, CA, USA: ADT 1.5.6) using the hybrid Lamarckian Genetic Algorithm (LGA) was used for performing molecular docking simulations as reported in the literature [13,14]. In short, the 3D crystal structures (resolution: 2.5 Å) of iNOS (PDB code: 3E6T) and COX-2 (PDB code: 1PXX) were obtained from the RCSB Protein Data Bank. The configurations of compounds 1 and 3 were determined by their nuclear overhauser effect spectroscopy (NOESY) spectra and time-dependent density functional theory (TDDFT) ECD calculations. Chem3D Pro 14.0 software (CambridgeSoft, Waltham, MA, USA) was used for construction of the standard 3D structures (PDB format) of compounds 1 and 3.

3. Results

3.1. Structure Elucidation of Compounds 1 and 2

Compound 1 was obtained as a dark brownish powder, and its molecular formula was identified as C₁₈H₁₄O₆ by HRESIMS (*m/z* 325.0714 [M–H][−]; calculated for C₁₈H₁₃O₆, 325.0712). It exhibited UV maxima at 262 nm and IR maxima at 3333, 1718, and 1524 cm^{−1}, suggesting the presence of a hydroxyl, ester group, and aromatic ring. The ¹³C NMR spectral data of compound 1 (Table 1) exhibited 18 carbon signals including a carbonyl carbon (δ_C 173.9), 12 aromatic carbons (from δ_C 115.7 to 145.9), an oxygenated methylene carbon (δ_C 72.4), a methine carbon (δ_C 42.3), and a methylene carbon (δ_C 29.0).

The remaining two quaternary carbons (δ_C 160.9 and 128.2) were derived from a double bond. The ¹H NMR spectrum revealed one 1,2,4,5-tetrasubstituted aromatic ring [δ_H 6.72 (s, H-6) and 6.60 (s, H-3)], and the one 1,3,4-trisubstituted aromatic ring [δ_H 6.63 (d, *J* = 8.0, H-5'), 6.59 (d, *J* = 2.0, H-2'), and 6.45 (dd, *J* = 8.0 and 2.0, H-6')], an oxygenated methylene [δ_H 4.97 (d, *J* = 17.0) and 4.89 (d, *J* = 17.5), H-9], a methine [δ_H 4.53 (s, H-7')], and a methylene [δ_H 3.86 (d, *J* = 23.0) and 3.62 (overlapped), H-7]. The heteronuclear multiple bond correlation spectroscopy (HMBC) correlations of 1 (Figure 2) suggest aryltetralin lactone type lignan with a double bond at C-8 and C-8'.

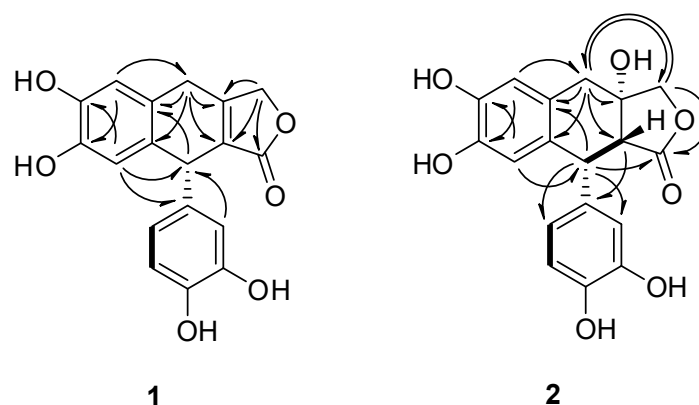


Figure 2. Selected correlations of compounds **1** and **2**: correlation spectroscopy (COSY, ---) and heteronuclear multiple bond correlation spectroscopy (HMBC, ---) (in acetone- d_6 and methanol- d_4).

The absolute configuration at C-7' of compound **1** was established by comparing its experimental ECD spectrum with those calculated spectra of (7'*R*) and (7'*S*) models using the time-dependent density functional theory (TDDFT) method. The experimental ECD spectrum of compound **1** exhibited a positive Cotton effect (CE) at 239 nm ($\Delta\epsilon +2.1$) and negative CEs at 214 nm ($\Delta\epsilon -10.4$) and 254 nm ($\Delta\epsilon -5.3$). The experimental data (Figure 3) was in agreement with the calculated ECD spectrum of the (7'*R*) model, suggesting the absolute configuration of compound **1** as (7'*R*). Thus, the structure of **1** was elucidated as (*R*)-9-(3, 4-dihydroxyphenyl)-6,7-dihydroxy-4,9-dihydronaphtho[2'-C-c]furan-1(3*H*)-one, and was named as petasitesin A.

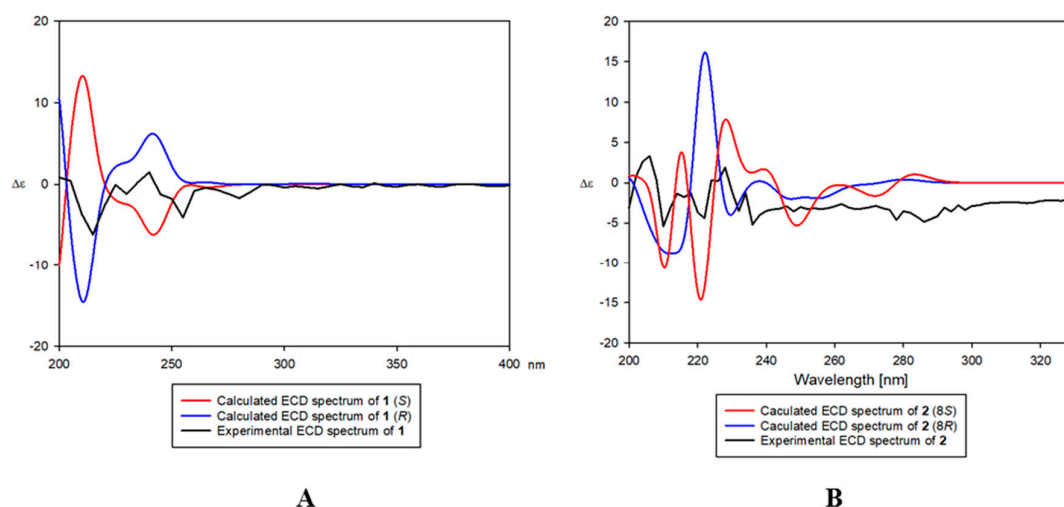


Figure 3. Comparison of experimental and calculated electronic circular dichroism (ECD) spectra of compounds **1** (A) and **2** (B).

The compound **2** was isolated as a dark brownish powder. Its molecular formula was established as $C_{18}H_{16}O_7$ by HRESIMS (m/z 343.0810 $[M-H]^-$; calculated for $C_{18}H_{15}O_7$, 343.0818). The 1H and ^{13}C NMR data of **2** were similar to those of **1** (Table 1), although the NMR solvents were different from each other due to the different solubility of the compounds. Comparison of the ^{13}C NMR data and molecular weights from **1** and **2** suggested that the carbons C-8 and C-8' of **1** with a double bonded linkage (δ_C 160.9 and 128.2) were replaced by an oxygenated quaternary (δ_C 78.0) and methine (δ_C 56.2) carbon atoms. The correlation spectroscopy (COSY) correlation between H-7' (δ_H 4.18) and H-8' (δ_H 3.24), and the HMBC experiment revealed aryltetralin lactone type lignan (Figure 4). Considering a biogenetic relationship with **1**, the absolute configuration at C-7' of **2** was suggested to be (*R*)-configuration [15].

The coupling constant of 3.0 Hz between H-7' and H-8' suggested the *cis*-geometry of C-7' and C-8'. It was further confirmed by the NOESY interaction of H-7' and H-8' [16].

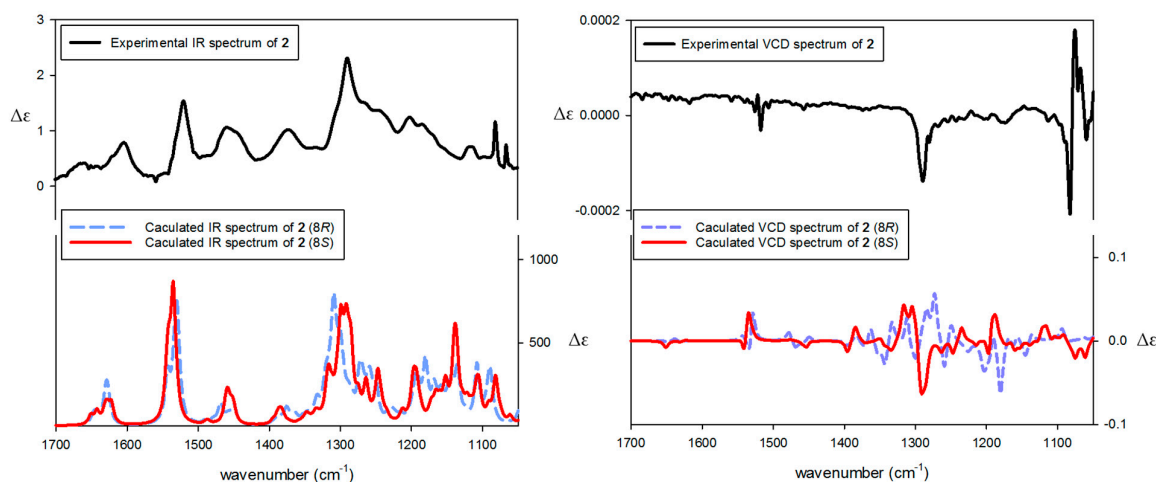


Figure 4. Comparison of experimental and calculated vibrational circular dichroism (VCD) spectra of compound **2** (*c* 0.5 M, DMSO-*d*₆).

To determine the absolute configuration C-8 of **2**, experimental ECD spectrum of **2** was compared with the calculated spectra of (8*R*,7'*R*,8'*R*) and (8*S*,7'*R*,8'*R*) models using the TDDFT method. The experimental ECD spectrum of **2** showed positive CEs at 203 nm ($\Delta\epsilon$ +4.0) and 229 nm ($\Delta\epsilon$ +1.9), and negative CEs at 210 nm ($\Delta\epsilon$ -5.4) and 222 nm ($\Delta\epsilon$ -4.4). The experimental spectrum (Figure 3) was also in agreement with the calculated ECD spectrum of (8*S*,7'*R*,8'*R*) model. Moreover, the VCD spectrum of **2** was measured additionally to establish the configuration at C-8. The conformity of the experimental IR and VCD spectra and theoretical spectra of **2** suggested the absolute configuration of **2** as (8*S*,7'*R*,8'*R*) (Figure 4). Therefore, the structure of **2** was proposed as (9*R*,3*aS*,9*aR*)-9-(3,4-dihydroxyphenyl)-6,7,3*a*-trihydroxy-4,9,3*a*,9*a*-tetrahydronaphtho[2,3-*c*]furan-1(3*H*)-one, and was named as petasitesin B.

Compounds **3–8** were identified as cimicifugic acid D (**3**) [17], fukinolic acid (**4**) [7], 3,4-dicaffeoylquinic acid (**5**) [18], 3,5-dicaffeoylquinic acid (**6**) [18], 4,5-dicaffeoylquinic acid (**7**) [18], and caffeic acid (**8**) [19] by comparison of their NMR data with those reported.

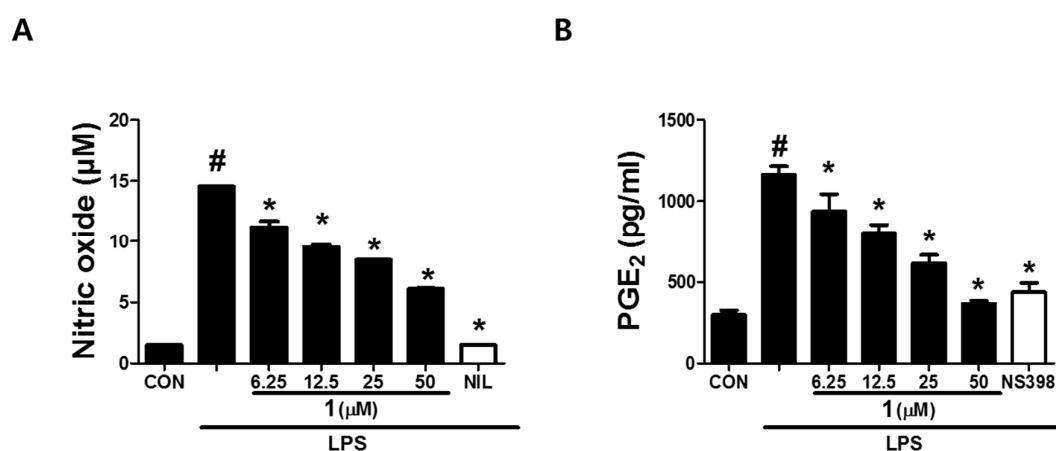
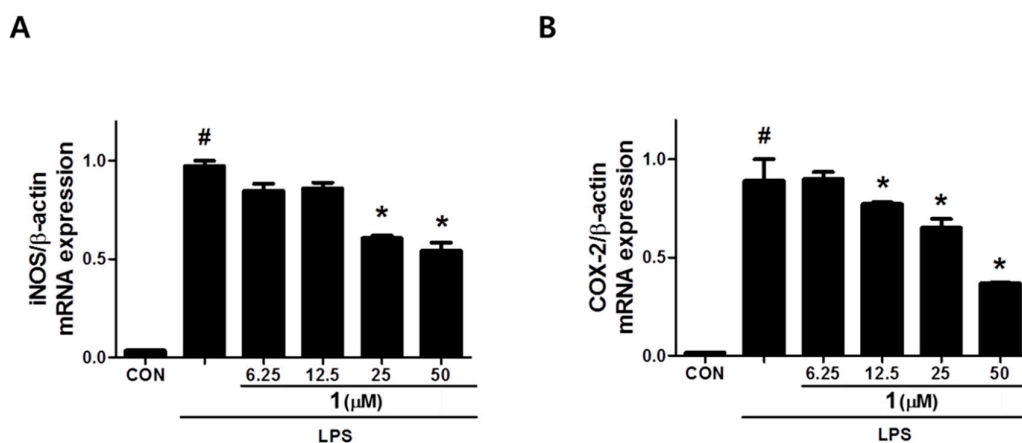
3.2. Anti-inflammatory Effects of the Isolates

As shown in Table 2, cimicifugic acid D (**3**) and the new compound **1** (petasitesin A) exhibited significant inhibitory activities against NO production with IC₅₀ values of 12 ± 1.1 and 15 ± 1.4 μM, respectively, without affecting the cell viability (Figure S15). 4,5-Dicaffeoylquinic acid showed mild activity with an observed IC₅₀ value of 38.9 ± 0.72 μM. On the other hand, compound **1** showed the most potent inhibitory effect on PGE₂ production with an IC₅₀ value of 17 ± 3.2 μM (Table 2) in a dose-dependent manner (Figure 5). These results suggest that compound **1** might have an anti-inflammatory effect due to inhibition of the production of NO and PGE₂ which are the key inflammatory mediators of macrophages. It is worth noting that compound **1** significantly suppressed the expression of NO and PGE₂ synthesis enzymes, inducible nitric oxide synthase (iNOS) and cyclooxygenase-2 (COX-2), respectively (Figure 6), in a concentration-dependent manner. The data indicate that the inhibitory effect of compound **1** on NO and PGE₂ production in macrophages is related to the regulation of iNOS and COX-2 expression.

Table 2. Inhibitory effects of the compounds from *P. japonicus* on NO and PGE₂ production in lipopolysaccharide (LPS)-induced RAW 264.7 cells.

Compound	IC ₅₀ (μM) ^a	
	NO	PGE ₂
1	15 ± 1.4	17 ± 3.2
2	>50	>50
Cimicifugic acid D (3)	12 ± 1.1	43 ± 7.9
4,5-Dicaffeoylquinic acid	38.9 ± 0.72	>50
Caffeic acid	>50	45.7 ± 0.87

^a The values represent the means of the results from three independent experiments with similar patterns. L-N⁶-(1-Iminoethyl)lysine (L-NIL) and N-[2-(cyclohexyloxy)-4-nitrophenyl]methanesulfonamide (NS-398) were used as a positive control substance for NO [half maximal inhibitory concentration IC₅₀ value = 1.62 ± 0.08 μM] and prostaglandin E₂ (PGE₂) productions (IC₅₀ value = 3.3 ± 0.15 μM), respectively. Three known compounds, fukinolic acid, 3,4-dicaffeoylquinic acid, and 3,5-dicaffeoylquinic acid were inactive (IC₅₀ value > 50 μM) in this assay system.

**Figure 5.** Effects of compound 1 (6.25, 12.5, 25 or 50 μM) on LPS-stimulated NO (A) and PGE₂ (B) productions in RAW 264.7 macrophages. #: $p < 0.05$ as compared with the untreated group, *: $p < 0.05$ as compared with the LPS only-treated group.**Figure 6.** Effect of compound 1 on the expression of iNOS (A) and COX-2 (B) in RAW 264.7 macrophages. #: $p < 0.05$ as compared with the untreated group, *: $p < 0.05$ as compared with the LPS only-treated group.

To better understand the molecular mechanism of inhibitory activities against NO and PGE₂ production, the most active compounds 1 and 3 were subjected to molecular docking studies. The results showed that 1 and 3 had strong affinities with both NO and PGE₂ synthesis enzymes, iNOS and COX-2 (Figure 7, Table 3). The binding residues and logarithms of free binding energy are given in Table 3. These results implicated that 1 and 3 may directly interact with the cavity residues of

iNOS and COX-2, leading to the activity reduction of free iNOS and COX-2 enzymes. Taken together, these results indicate petasitesin A (**1**), a novel lignan isolated from butterbur leaves extract, exhibits anti-inflammatory properties by suppressing NO and PGE₂ production via inhibiting the expression of iNOS and COX-2 and binding to the free iNOS and COX-2 enzymes.

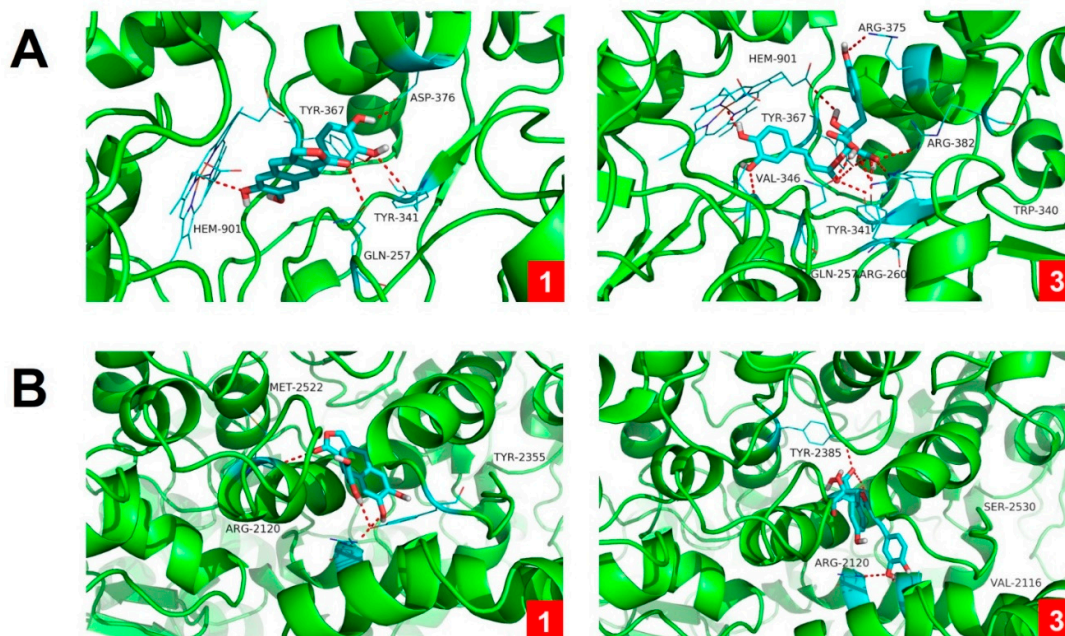


Figure 7. Molecular docking results of compounds **1** and **3** with iNOS (**A**) and COX-2 (**B**) enzymes. Molecular docking simulations obtained at the lowest energy conformation, highlighting potential hydrogen contacts of **1** and **3**, respectively (nitrogen is blue; oxygen is red; carbon is cyan; hydrogen is gray). For clarity, only interacting residues are labeled. Hydrogen bonding interactions are shown by dashes. These figures were created by PyMOL (Schrödinger, LLC, New York, NY, USA: version 1.3).

Table 3. Logarithms of free binding energies (FBE, kcal/mol) of NO inhibitors to the active cavities of iNOS (PDB Code: 3E6T) and COX-2 (PDB code: 1PXX) and targeting residues of the binding site located on the mobile flap.

Compound	−Log (FBE)		Targeting Residues	
	iNOS	COX-2	iNOS	COX-2
1	−8.8	−7.5	ASP-376, TYR-367, TYR-341, GLN-257, HEM-901	ARG-2120, TYR-3355, MET-2522
3	−10.0	−8.3	ARG-260, ARG-375, ARG-382, TYR-341, TYR-367, TRP-340, GLN-257, HEM-901, VAL-346	ARG-2120, TYR-2385, VAL-2116, SER-2530

4. Discussion

In the present study, we isolated two new aryltetralin lactone lignans, petasitesin A and B (**1** and **2**) from the leaves of *P. japonicus*. To the best of our knowledge, this is the first report on the isolation of the aryltetralin lactone type lignans from the leaves of *P. japonicas*. Although cimicifugic acid D (**3**) has been isolated from *Cimicifuga* spp. including black cohosh (*Cimicifuga racemosa*) and possesses vasoactive effect and hyaluronidase inhibitory activity [20,21], this is the first finding that it presents in *P. japonicus* and inhibits pro-inflammatory mediators, NO and PGE₂.

A new lignan petasitesin A (**1**) showed a potent inhibitory effect on the production of both NO and PGE₂ in LPS-stimulated macrophages (IC₅₀ values < 20 μM). Our molecular docking

studies reveal that petasitesin A (**1**) can interact with the cavity residues of both iNOS and COX-2. Interestingly, petasitesin A (**1**) also inhibited the mRNA expression of iNOS and COX-2 induced by LPS in macrophages. However, the molecular mechanism of action underlying the gene expression regulation by petasitesin A remains to be investigated. Considering that LPS binds to toll-like receptor 4 (TLR4), the TLR4-mediated NF- κ B pathway is likely associated with the inhibition of iNOS and COX-2 expression by petasitesin A. In fact, NF- κ B is a key transcriptional factor to regulate the iNOS and COX-2 gene in macrophages under the inflammatory condition. In this regard, the effect of petasitesin A on the NF- κ B pathway can be further elucidated.

5. Conclusions

New lignans (compounds **1** and **2**) and six known compounds were isolated and identified from the leaves of *P. japonicus*. Petasitesin A (**1**) and cimicifugic acid D (**3**) inhibit production of inflammatory mediators NO and PGE₂. Petasitesin A (**1**) inhibits iNOS and COX-2 expression, and petasitesin A (**1**) and cimicifugic acid D (**3**) have strong affinities with both iNOS and COX-2 enzymes in molecular docking studies. Thus, petasitesin A (**1**) and cimicifugic acid D (**3**) are worthy of further pharmacological evaluation for their potential as anti-inflammatory drugs.

Supplementary Materials: The following are available online at <http://www.mdpi.com/2218-273X/9/12/806/s1>, Figure S1: HR-ESI-MS spectrum of compound **1**, Figure S2: The ¹H-NMR (500 MHz, CD₃COCD₃) spectrum of compound **1**, Figure S3: The ¹³C-NMR (125 MHz, CD₃COCD₃) spectrum of compound **1**, Figure S4: The HSQC spectrum of compound **1** in CD₃COCD₃, Figure S5: The COSY spectrum of compound **1** in CD₃COCD₃, Figure S6: The HMBC spectrum of compound **1** in CD₃COCD₃, Figure S7: The NOESY spectrum of compound **1** in CD₃COCD₃, Figure S8: HR-ESI-MS spectrum of compound **2**, Figure S9: The ¹H-NMR (500 MHz, CD₃OD) spectrum of compound **2**, Figure S10: The ¹³C-NMR (125 MHz, CD₃OD) spectrum of compound **2**, Figure S11: The HSQC spectrum of compound **2** in CD₃OD, Figure S12: The COSY spectrum of compound **2** in CD₃OD, Figure S13: The HMBC spectrum of compound **2** in CD₃OD, Figure S14: The NOESY spectrum of compound **2** in CD₃OD, Figure S15: Cell viability of the isolates from *P. japonicus*.

Author Contributions: D.L. and D.S.J. conceived and designed the experiments; J.S.L., M.J., S.P., S.M.R., and Z.S. performed the experiments; J.S.L. and S.M.R. analyzed the data; J.L., Y.G., and J.-H.C. interpreted the data and contributed to manuscript structure and flow; and J.S.L., M.J., and Z.S. wrote the paper. All authors reviewed and confirmed the manuscript.

Funding: This research was supported by Korea Institute of Planning and Evaluation for Technology in Food, Agriculture and Forestry (IPET) through Agri-Bio Industry Technology Development Program, funded by Ministry of Agriculture, Food and Rural Affairs (MAFRA), Republic of Korea (116044-1, 118046-03). This work was also supported by the National Research Foundation of Korea (NRF) grant funded by Ministry of Science and ICT (MSIT), Republic of Korea (NRF-2019R1A2C1083945).

Conflicts of Interest: The authors declare no conflict of interest.

References

1. Kusano, A.; Seyama, Y.; Nagai, M.; Shibano, M.; Kusano, G. Effects of fukinolic acid and cimicifugic acids from *Cimicifuga* species on collagenolytic activity. *Biol. Pharm. Bull.* **2001**, *24*, 1198–1201. [[CrossRef](#)] [[PubMed](#)]
2. Mizushima, Y.; Ishidoh, T.; Kamisuki, S.; Nakazawa, S.; Takemura, M.; Sugawara, F.; Yoshida, H.; Sakaguchi, K. Flavonoid glycoside: A new inhibitor of eukaryotic DNA polymerase α and a new carrier for inhibitor-affinity chromatography. *Biochem. Biophys. Res. Commun.* **2003**, *301*, 480–487. [[CrossRef](#)]
3. Naya, K.; Hayashi, M.; Takagi, I.; Nakamura, S.; Kobayashi, M. The structural elucidation of sesquiterpene lactones from *Petasites japonicus* Maxim. *Bull. Chem. Soc. Jpn.* **1972**, *45*, 3673–3685. [[CrossRef](#)]
4. Tori, M.; Kawahara, M.; Sono, M. Eremophilane-type sesquiterpenes from fresh rhizomes of *Petasites japonicus*. *Phytochemistry* **1997**, *47*, 401–409. [[CrossRef](#)]
5. Wang, S.; Jin, D.Q.; Xie, C.; Wang, H.; Wang, M.; Xu, J.; Guo, Y. Isolation, characterization, and neuroprotective activities of sesquiterpenes from *Petasites japonicus*. *Food Chem.* **2013**, *141*, 2075–2082. [[CrossRef](#)] [[PubMed](#)]
6. Shimoda, H.; Tanaka, J.; Yamada, E.; Morikawa, T.; Kasajima, N.; Yoshikawa, M. Anti type I allergic property of Japanese butterbur extract and its mast cell degranulation inhibitory ingredients. *J. Agric. Food Chem.* **2006**, *54*, 2915–2920. [[CrossRef](#)] [[PubMed](#)]

7. Sakamura, S.; Yoshihara, T.; Toyoda, K. The constituents of *Petasites japonicus*: Structures of fukiic acid and fukinolic acid. *Agric. Biol. Chem.* **1973**, *37*, 1915–1921. [[CrossRef](#)]
8. Jeong, M.; Kim, H.M.; Kim, H.J.; Choi, J.H.; Jang, D.S. Kudsuphilactone B, a nortriterpenoid isolated from *Schisandra chinensis* fruit, induces caspase-dependent apoptosis in human ovarian cancer A2780 cells. *Arch. Pharm. Res.* **2017**, *40*, 500–508. [[CrossRef](#)]
9. Du, Y.E.; Lee, J.S.; Kim, H.M.; Ahn, J.H.; Jung, I.H.; Ryu, J.H.; Choi, J.H.; Jang, D.S. Chemical constituents of the roots of *Codonopsis lanceolata*. *Arch. Pharm. Res.* **2018**, *41*, 1082–1091. [[CrossRef](#)]
10. Kwon, J.; Lee, H.; Ko, W.; Kim, D.C.; Kim, K.W.; Kwon, H.C.; Guo, Y.; Sohn, J.H.; Yim, J.H.; Kim, Y.C.; et al. Chemical constituents isolated from Antarctic marine-derived *Aspergillus* sp. SF-5976 and their anti-inflammatory effects in LPS-stimulated RAW 264.7 and BV2 cells. *Tetrahedron* **2017**, *73*, 3905–3912. [[CrossRef](#)]
11. Ryu, S.M.; Lee, H.M.; Song, E.G.; Seo, Y.H.; Lee, J.; Guo, Y.; Kim, B.S.; Kim, J.J.; Hong, J.S.; Ryu, K.H.; et al. Antiviral activities of trichothecenes isolated from *Trichoderma albolutelescens* against pepper mottle virus. *J. Agric. Food. Chem.* **2017**, *65*, 4273–4279. [[CrossRef](#)] [[PubMed](#)]
12. Shin, J.S.; Lee, K.G.; Lee, H.H.; Lee, H.J.; An, H.J.; Nam, J.H.; Jang, D.S.; Lee, K.T. α -Solanine Isolated from *Solanum Tuberosum*, L. cv Jayoung Abrogates LPS-Induced Inflammatory Responses Via NF- κ B Inactivation in RAW 264.7 Macrophages and Endotoxin-Induced Shock Model in Mice. *J. Cell. Biochem.* **2016**, *117*, 2327–2339. [[CrossRef](#)] [[PubMed](#)]
13. Ma, J.; Ren, Q.; Dong, B.; Shi, Z.; Zhang, J.; Jin, D.Q.; Xu, J.; Ohizumi, Y.; Lee, D.; Guo, Y. NO inhibitory constituents as potential anti-neuroinflammatory agents for AD from *Blumea balsamifera*. *Bioorg. Chem.* **2018**, *76*, 449–457. [[CrossRef](#)] [[PubMed](#)]
14. Liu, F.; Yang, X.; Ma, J.; Yang, Y.; Xie, C.; Tuerhong, M.; Jin, D.Q.; Xu, J.; Lee, D.; Ohizumi, Y.; et al. Nitric oxide inhibitory daphnane diterpenoids as potential anti-neuroinflammatory agents for AD from the twigs of *Trigonostemon thyrsoides*. *Bioorg. Chem.* **2017**, *75*, 149–156. [[CrossRef](#)]
15. Won, T.H.; Song, I.H.; Kim, K.H.; Yang, W.Y.; Lee, S.K.; Oh, D.C.; Oh, W.K.; Oh, K.B.; Shin, J. Bioactive metabolites from the fruits of *Psoralea corylifolia*. *J. Nat. Prod.* **2015**, *78*, 666–673. [[CrossRef](#)]
16. Liu, Y.; Young, K.; Rakotondraibe, L.H.; Brodie, P.J.; Wiley, J.D.; Cassera, M.B.; Callmander, M.W.; Rakotondrajaona, R.; Rakotobe, E.; Rasamison, V.E.; et al. Antiproliferative compounds from *Cleistanthus boivinianus* from the Madagascar dry forest1. *J. Nat. Prod.* **2015**, *78*, 1543–1547. [[CrossRef](#)]
17. Takahira, M.; Kusano, A.; Shibano, M.; Kusano, G.; Miyase, T. Piscidic acid and fukiic acid esters from *Cimicifuga simplex*. *Phytochemistry* **1998**, *49*, 2115–2119. [[CrossRef](#)]
18. Wu, Q.Z.; Zhao, D.X.; Xiang, J.; Zhang, M.; Zhang, C.F.; Xu, X.H. Antitussive, expectorant, and anti-inflammatory activities of four caffeoylquinic acids isolated from *Tussilago farfara*. *Pharm. Biol.* **2016**, *54*, 1117–1124. [[CrossRef](#)]
19. Park, H.Y.; Nam, M.H.; Lee, H.S.; Jun, W.; Hendrich, S.; Lee, K.W. Isolation of caffeic acid from *Perilla frutescens* and its role in enhancing γ -glutamylcysteine synthetase activity and glutathione level. *Food Chem.* **2010**, *119*, 724–730. [[CrossRef](#)]
20. Noguchi, M.; Nagai, M.; Koeda, M.; Nakayama, S.; Sakurai, N.; Takahira, M.; Kusano, G. Vasoactive effects of cimicifugic acids C and D, and fukinolic acid in cimicifuga rhizome. *Biol. Pharm. Bull.* **1998**, *21*, 1163–1168. [[CrossRef](#)]
21. Iwanaga, A.; Kusano, G.; Warashina, T.; Miyase, T. Hyaluronidase inhibitors from “*Cimicifugae Rhizoma*” (a mixture of the rhizomes of *Cimicifuga dahurica* and *C. heracleifolia*). *J. Nat. Prod.* **2010**, *73*, 573–578. [[CrossRef](#)] [[PubMed](#)]

